

Realization of Maximum 2 A/mm Drain Current on Top-Gate Atomic-Layer-Thin Indium Oxide Transistors by Thermal Engineering

Pai-Ying Liao¹, Mengwei Si¹, Zhuocheng Zhang¹, Zehao Lin¹, and Peide D. Ye¹, *Fellow, IEEE*

Abstract—In this work, we demonstrate the record high maximum drain current (I_D) of 2 A/mm of top-gate (TG) indium oxide (In_2O_3) transistors. The scaled and atomic-layer-deposited (ALD) In_2O_3 transistors have channel length (L_{ch}) down to 40 nm and channel thickness (T_{ch}) down to 1.3 nm. Besides, the thermal budget of the whole material formation and device fabrication process is as low as 225 °C, making it compatible with back-end-of-line (BEOL) technologies by a huge margin. On the other hand, highly resistive silicon is utilized to serve as a desired high thermal conducting substrate to dissipate the generated heat efficiently as a larger current is conducted under a larger voltage bias. It greatly alleviates the self-heating effect (SHE) and allows an approximately 100% higher drain current. Quantitative studies of the SHE and channel temperature at ON-state with SiO_2/Si and highly resistive silicon substrates are also presented.

Index Terms—Atomic layer deposition, back-end-of-line (BEOL), oxide semiconductor.

I. INTRODUCTION

BEING widely applied as channel materials for thin-film transistors (TFTs) and potentially for back-end-of-line (BEOL) compatible monolithic 3-D integration, oxide semiconductors have received extensive attention and been broadly explored in the past years [1]–[9]. Among them, indium oxide (In_2O_3) [1]–[3] and doped indium oxides [4]–[8] are even of great interest because of their exceptional properties including high growth scalability and reproducibility to enable mass production, atomically smooth roughness to guarantee the surface quality, ambient stability to achieve little material degradation in air, and low thermal budget to be well suited with BEOL technologies.

Given its roughly 2.7-eV bandgap [9], In_2O_3 as an oxide semiconductor has attracted revived attention as a

promising channel material. Especially, the conformal growth of the atomic-layer-deposited (ALD) In_2O_3 enables it to form on uneven surfaces including sidewalls and deep trenches, which dramatically benefits the monolithic 3-D integration [1], [2], [10]–[13]. Moreover, another superiority of ALD is the ultrathin film growth and the precise thickness control down to the angstrom scale. It is known that as the physical size of transistors in integrated circuits becomes smaller according to Moore’s law, electrostatic control of the devices begins to lose. To maintain the controllability, natural length (proportional to the square root of T_{ch}) shorter than one-third of the L_{ch} , indicating an ultrathin channel, is favored [14]. Nonetheless, for ultrathin-body silicon devices, the mobility descends drastically with a power of six to the thickness [15], resulting in the low current density with the atomically thin channel such as 1–2 nm. Therefore, it requires a higher current density around this thickness range for a single device to conduct enough current. It has been reported that scaled back-gate (BG) In_2O_3 transistors accomplish channel thickness (T_{ch}) down to 0.7 nm [1] and drain current (I_D) up to 2.2 A/mm in enhancement mode as 1.5-nm-thick In_2O_3 acts as the channel [3], [16], qualifying In_2O_3 as a candidate material which has advantages in the ultrathin-body transistors.

However, the investigations of the In_2O_3 devices mostly focus on BG structure [1]–[3], and top-gate (TG) In_2O_3 transistors are rarely explored. On the other hand, TG devices are particularly demanded in many practical integration applications. The challenges for TG devices are due to 1) the performance degradation of the In_2O_3 channel after the growth of the high- κ oxide gate dielectric and 2) the drastic self-heating effect (SHE) as the current density becomes higher under high voltage biases. For the former, it is proposed that the oxygen atoms in the In_2O_3 layer are lost and taken away as the ALD hafnium oxide (HfO_2) is formed, which intensely generates more oxygen vacancies in the In_2O_3 channel and increases the OFF-state current value [17]. Fortunately, this is resolvable by lowering the growth temperature of HfO_2 from 200 °C to 120 °C followed by a low-temperature rapid-thermal-annealing (RTA) treatment in an O_2 environment. This method makes the TG In_2O_3 devices gate-tunable; however, the maximum I_D reaches only 570 mA/mm [17] because of the thermal issue. In addition, the high channel temperature might even result in the damage of the gate dielectric and the diminishing of the long-term reliability [18], [19]. To address this, thermal engineering which has been applied to other materials [20]–[22] might be a solid solution.

Therefore, we herein realize ALD-based TG In_2O_3 transistors achieving I_D as high as 2 A/mm by employing highly resistive silicon substrate to minimize SHE. In the previous

Manuscript received October 4, 2021; revised October 30, 2021; accepted November 3, 2021. Date of publication November 17, 2021; date of current version December 29, 2021. This work was supported in part by the Semiconductor Research Corporation (SRC), Nanoelectronic Computing REsearch (nCORE), the Innovative Materials and Processes for Accelerated Compute Technologies (IMPACT) Center, in part by the SRC/Defense Advanced Research Projects Agency (DARPA), the Joint University Microelectronics Program (JUMP), the Applications and Systems Driven Center for Energy-Efficient Integrated Nanotechnologies (ASCENT) Center. The review of this article was arranged by Editor J. F. Conley. (Corresponding author: Peide D. Ye.)

The authors are with the Birck Nanotechnology Center and the School of Electrical and Computer Engineering, Purdue University, West Lafayette, IN 47907 USA (e-mail: yep@purdue.edu).

Color versions of one or more figures in this article are available at <https://doi.org/10.1109/TED.2021.3125923>.

Digital Object Identifier 10.1109/TED.2021.3125923

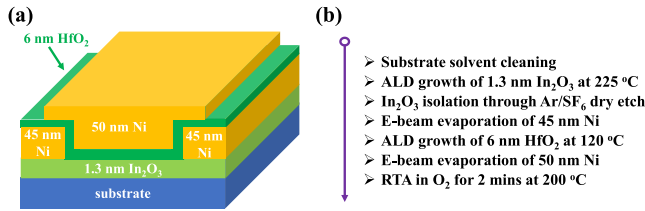


Fig. 1. (a) Schematic and (b) workflow of the fabrication process of a TG In_2O_3 transistor. The substrate is either 90-nm thermally grown SiO_2 on silicon or highly resistive silicon (resistivity $\sim 10^5 \Omega \cdot \text{cm}$).

exploration [1]–[3], silicon dioxide on silicon (SiO_2/Si) is usually chosen as the substrate due to its insulating property and vast commercial availability. Nevertheless, the thermal conductivity of silicon ($\kappa = 142 \text{ W} \cdot \text{m}^{-1} \cdot \text{K}^{-1}$) [23] is approximately 100 times higher than SiO_2 ($\kappa = 1.1 \text{ W} \cdot \text{m}^{-1} \cdot \text{K}^{-1}$) [24], implying that the generated heat can be dissipated much more efficiently from the bottom as silicon serves as the substrate. In this case, we utilize highly resistive silicon (resistivity $\sim 10^5 \Omega \cdot \text{cm}$) to block the leakage current through the substrate. Additionally, to estimate and compare the rough temperature of the channel with different substrates as a certain amount of current flows through, we measure the regression of the transconductance (g_m) of In_2O_3 TG transistors from room temperature to 160°C as an approximate channel thermometer [25]–[28]. It is revealed that the In_2O_3 on SiO_2 is already heated up to 140°C locally while the silicon devices are still under 40°C in the same condition. The enormous thermal conductivity difference benefits the realization of scaled TG In_2O_3 transistors with high current carrying capacity up to a maximum I_D of 2 A/mm.

II. EXPERIMENTS

Fig. 1 illustrates the schematic view of a TG In_2O_3 transistor and the workflow of the fabrication. From bottom to top, the stacks are substrate (either 90-nm thermally grown SiO_2 on silicon or highly resistive silicon), isolated In_2O_3 channel with a thickness of 1.3 nm, 45-nm Ni serving as source and drain metal contacts, 6-nm HfO_2 of the gate dielectric, and 50-nm Ni acting as TG metal electrode.

Standard solvent cleaning steps are followed before the substrates are used in the device fabrication process. 1.3-nm of In_2O_3 thin film is deposited by ALD at 225°C with trimethylindium (TMIn) and H_2O as the In and O precursors, respectively, on the pre-cleaned substrates. The as-deposited In_2O_3 thin film is isolated through a dry-etch process with Ar/SF_6 plasma at room temperature. Then, 45-nm Ni as source and drain contacts are defined with variant L_{ch} by e-beam lithography, e-beam evaporation, and a lift-off process. On top of them, 6-nm HfO_2 is conformally formed by ALD at 120°C with $[(\text{CH}_3)_2\text{N}]_4\text{Hf}$ (TDMAHf) and H_2O as the Hf and O precursors, respectively. The relatively low temperature is chosen to minimize the interaction between In_2O_3 and the growth of HfO_2 to preserve the intrinsic properties of the channel semiconducting material [17] and dedicated ALD chambers are employed in order to prevent cross-contamination of In_2O_3 and HfO_2 deposition. 50-nm Ni serving as TG electrode is formed in the same way as the source and drain contacts. Last, the devices are treated with RTA in an O_2 environment at 200°C for 2 min to reduce the oxygen vacancies in the In_2O_3 channel induced by the ALD growth process of HfO_2 [17]. The whole fabrication process requires a thermal budget as

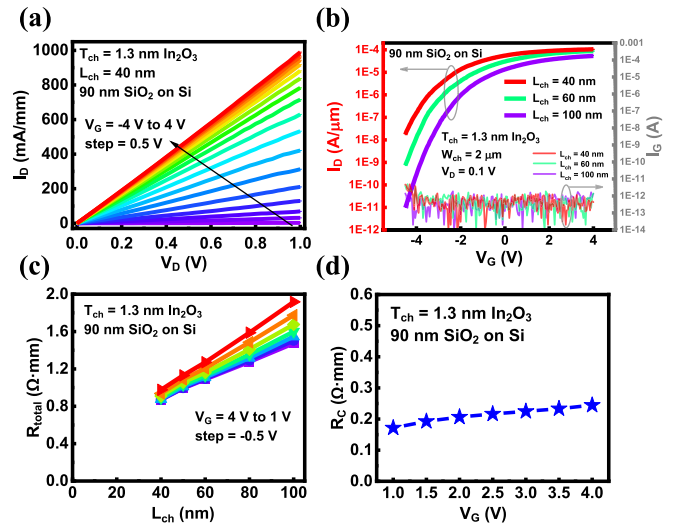


Fig. 2. (a) Output and (b) transfer characteristics of TG In_2O_3 transistors with SiO_2/Si substrate and L_{ch} of (a) 40 nm and (b) 40, 60, and 100 nm. (c) Total resistance of the devices with variant L_{ch} at ON-state for TLM extraction. (d) Extracted R_C values from (c) showing great contact between the In_2O_3 channel and source/drain contacts.

low as 225°C which is for the formation of the atomic-layer-thin In_2O_3 channel.

III. RESULTS AND DISCUSSION

Fig. 2(a) exhibits the output characteristics of a representative TG In_2O_3 transistor with L_{ch} of 40 nm, T_{ch} of 1.3 nm, W_{ch} of $2 \mu\text{m}$, 6-nm HfO_2 as the TG dielectric, SiO_2/Si as the substrate, and annealing at 200°C in an O_2 environment. The TG voltage (V_G) sweeps from -4 to 4 V with a 0.5-V step, and the maximum I_D achieves 991 mA/mm at V_G of 4 V and a drain voltage (V_D) of 1 V, which surpasses the highest reported value of 570 mA/mm for TG In_2O_3 transistors [17] to the best of our knowledge. Fig. 2(b) presents the transfer characteristics, showing an ON-OFF ratio of almost 4 to more than 6 orders with variant L_{ch} from 40 to 100 nm. The gate leakage currents are illustrated and much smaller than the drain currents. Some key parameters are extracted as follows, threshold voltage (V_T) being -1.1 , -1.8 , and -2.5 V, subthreshold swing being 344, 433, and 577 mV/dec for L_{ch} of 100, 60, and 40 nm, respectively, and field-effect mobility (μ_{FE}) being $4.1 \text{ cm}^2 \cdot \text{V}^{-1} \cdot \text{s}^{-1}$. For the devices with L_{ch} of 100, 60, and 40 nm, the maximum I_D of them are 405, 660, and 991 mA/mm, respectively, at V_G of 4 V and V_D of 1 V. It is noticeable that the I_D of the transistors at V_G of 4 V and V_D of 1 V is roughly proportional to the inverse of the L_{ch} , indicating that 1) the semiconducting In_2O_3 channel can be nicely scaled and 2) most of the resistance is contributed by the channel, that is, contact resistance (R_C) is reasonably low. To further explore the R_C of TG In_2O_3 devices at ON-state, the total resistances (R_{total}) with different L_{ch} and V_G from 4 to 1 V are extracted and arranged into Fig. 2(c) where R_{total} consists of 1) $2R_C$ designated to the contacts between the semiconducting channel and source/drain metal and 2) sheet resistance (R_{sh}) contributed by the channel material and proportional to the L_{ch} . In each case of V_G , the extracted data points are in a superb linear fashion, and therefore, the R_C is accordingly obtained by extrapolation with a traditional transfer length measurement (TLM) method [29]. The y-axis intersection with the extrapolated regression line is regarded

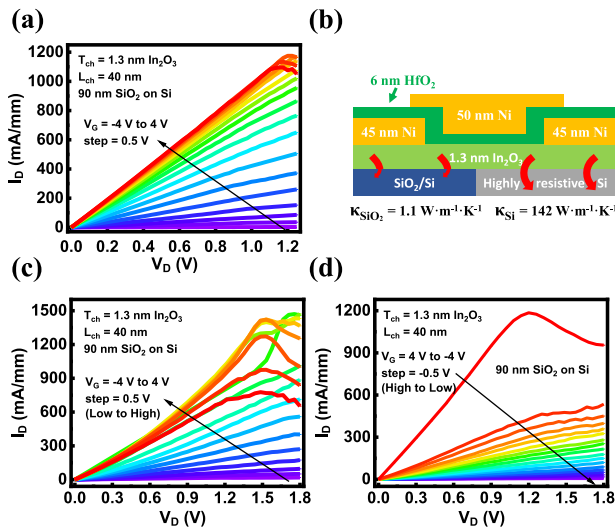


Fig. 3. (a) Degraded I_D curves of a TG In_2O_3 transistor with SiO_2/Si substrate and a large V_D up to 1.25 V, revealing the SHE. (b) Cross-sectional exhibition of the heat dissipation of In_2O_3 devices with different substrates. Silicon with around 100 times higher thermal conductivity is able to passivate the generated thermal energy much more efficiently. Drastically degenerated and extremely chaotic I_D - V_D curves with V_G sweeping (c) from low to high and (d) from high to low. The totally different behaviors imply that SHE is dominating over the transport performance.

as $2R_C$. Fig. 2(d) illustrates the acquired R_C under different V_G with the largest value of $0.24 \Omega \cdot \text{mm}$ at V_G of 4 V, which is still lower than the reported value of $0.36 \Omega \cdot \text{mm}$ [1] with a BG structure. The low R_C value implies that the In_2O_3 channel and the Ni source/drain are of satisfactory contact in the TG structure.

Even though TG In_2O_3 devices with SiO_2/Si substrates manifest I_D of roughly 1 A/mm, it is unable to achieve even higher as the BG transistors show up to 2.2 A/mm [3]. Fig. 3(a) reveals the difficulties as a larger V_D is applied. Noticeably, the curves of I_D start to saturate and then degrade while V_D of 1.25 V is kept applied with variant V_G sweeping, which is mostly ascribed to the SHE. As illustrated in Fig. 3(b), a large amount of heat could be generated when large current passes through the ultrathin In_2O_3 channel. Nevertheless, the device is not capable of dissipating the created thermal energy efficiently when SiO_2/Si serves as the substrate, causing dramatic elevation of the local temperature and the damage of the In_2O_3 channel. Under certain conditions, the transistors no longer behave well and are even unrecoverable. To further investigate the SHE, a larger V_D of 1.8 V is applied to two devices with one sweeping the V_G from low to high and the other one from high to low as exhibited in Fig. 3(c) and (d), respectively. The two situations reveal completely different results. Observably, in Fig. 3(c), the current degradation becomes more and more critical over the sweeps of larger V_G . The curves are entirely in an unexpected situation and the behavior becomes extremely unstable due to the severe SHE. The red color is chosen and utilized to imply the high-temperature condition. On the other hand, in Fig. 3(d), even the first curve already reveals poor performance with V_G of 4 V applied first. After the first measurement and thermal stress, the device is degraded significantly or partly damaged. All the following measurements show underscored performance. The limited capability of heat dissipation of the devices restricts themselves from broader applications. Note that similar SHE also exhibits on BG transistors [1]–[3].

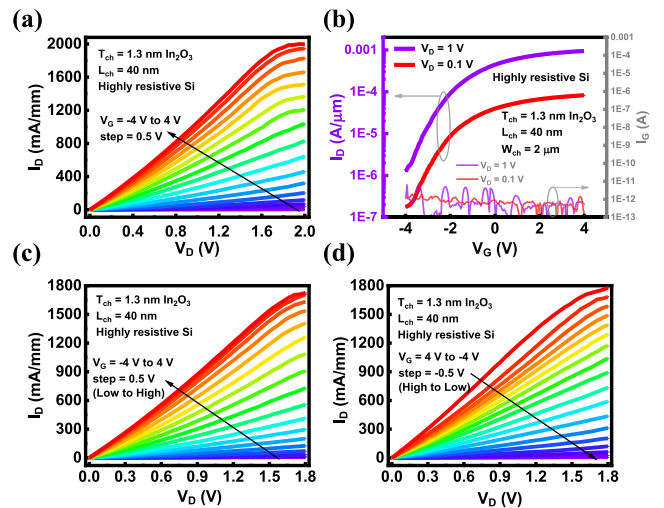


Fig. 4. (a) Output and (b) transfer characteristics of TG In_2O_3 transistors with highly resistive silicon substrate and L_{ch} of 40 nm. Cured I_D - V_D curves with V_G sweeping (c) from low to high and (d) from high to low.

To address this issue, a thermal management method is adopted. Highly resistive silicon (resistivity $\sim 10^5 \Omega \cdot \text{cm}$) is used to replace the SiO_2/Si substrate to assist in dissipating the generated thermal energy as large current is conducted. Silicon is chosen because of its much higher thermal conductivity of $142 \text{ W} \cdot \text{m}^{-1} \cdot \text{K}^{-1}$ [23] compared with that of SiO_2 $1.1 \text{ W} \cdot \text{m}^{-1} \cdot \text{K}^{-1}$ [24], the widely commercial availability, and the great affordability. Fig. 4(a) illustrates the output characteristics of a TG In_2O_3 device with highly resistive silicon as the substrate, the same L_{ch} of 40 nm, T_{ch} of 1.3 nm, 6-nm of HfO_2 as the TG dielectric, and 200°C RTA in an O_2 environment. The only difference is the substrate in operation. Even with V_D of 2 V applied, the created heat can be majorly dissipated ascribed to the high thermal conductivity of silicon. Consequently, the critical SHE is considerably mitigated, and the device achieves a much higher I_D of 2 A/mm at V_D of 2 V and V_G of 4 V. The 2 A/mm value is around 100% higher than that of 0.99 A/mm with SiO_2/Si substrate. Fig. 4(b) exhibits the transfer characteristics of the device. It performs roughly three orders of ON-OFF ratio, which is close to that of SiO_2/Si in Fig. 2(b). To compare the SHE in the two cases, alike Fig. 3(c) and (d), V_D of 1.8 V is applied to two In_2O_3 transistors with one sweeping the V_G from low to high and the other one from high to low. In Fig. 4(c), decent output curves are obtained. Unlike Fig. 3(c) exhibiting the dramatic current descent, Fig. 4(c) shows much healed SHE only with the utmost two curves being close. Similarly, in Fig. 4(d), even though the difference between the topmost two curves is a little larger, the severe SHE is greatly eliminated compared with Fig. 3(d) whose I_D degrades drastically within and after the first curve. With the huge discrepancies between Figs. 3(c) and (d) and 4(c) and (d), it is direct and unambiguous evidence that substituting the SiO_2/Si substrate with highly resistive silicon in TG In_2O_3 transistors largely reduces the SHE and observably benefits its transport performance.

In order to further quantitatively explore the SHE on the TG In_2O_3 device behavior, the current conducted through the transistors at ON-state with the two different substrates is measured ten times in a row. Because of the SHE, the local temperature at the In_2O_3 channel will increase after each measurement and degrade the channel mobility and contacts, which leads to performance degradation in the following

measurements. The same dimensional parameters of 40-nm L_{ch} , 1.3-nm T_{ch} , and 6-nm HfO_2 are utilized, and V_G of 4 V is chosen to ensure the entire experimental setup to be the same. Fig. 5(a)–(d) illustrates the ten collections of I_D curves with SiO_2/Si substrate and variant V_D applied where individual transistors with the same structure are employed in each subfigure. The V_D in Fig. 5(a) is only 0.5 V, and all the ten curves overlap with each other, meaning that no SHE takes place. The V_D in Fig. 5(b) is elevated to 0.8 V, and the curves start to decrease one time after another with around a 9% reduction in the tenth test compared to the first. The V_D applied in Fig. 5(c) is further enlarged to 1.0 V, and the distinctions between the curves become more obvious, indicating that SHE is deteriorating the electric behavior. The V_D in Fig. 5(d) is up to 1.8 V, and the performance in the first collection is already damaged, specifying the acute SHE. Moreover, the current degrades radically in the following measurements, and the I_D is decreased by approximately 77% compared to the first collection with the tenth. It is observable that the few topmost curves in this figure are principally similar to the ones in Fig. 3(d), implying that the SHE partly damages the device permanently as large V_G is applied first. Besides, it also verifies the reproducibility of the experiments and the consistency of the setup and devices. In great contrast to Fig. 5(d), Fig. 5(e) illustrates V_D of 1.8 V with silicon as the substrate. Observably, the SHE is mostly cured, and only a little degradation remains. The current deterioration between the first and the tenth measurement is only 7.5% which is even better than the case of V_D of 0.8 V with SiO_2/Si . The comparison of the degeneration over the ten collections between the two different substrates is arranged in Fig. 5(f), and the descending rate of highly resistive silicon substrate devices is less than 10% of the SiO_2/Si ones. The satisfactory capacity of heat dissipation of silicon considerably alleviates the serious SHE suffering SiO_2 and profits the exceptional I_D of 2 A/mm for TG In_2O_3 devices.

Besides, to roughly estimate the local temperature of the In_2O_3 channel as operating at ON-state in a quantitative way, the changes of the transconductance (g_m) under variant chuck temperature up to 160 °C are statistically investigated with SiO_2/Si serving as the substrate [25]–[27]. The g_m values here are extracted from I_D – V_G measurements at V_G around 4 V. A long L_{ch} of 1 μm and a low V_D of 50 mV are chosen to minimize the produced heat by the devices during the measurements. It is shown previously in Fig. 5(a) and discussed above that the SHE at V_D of 500 mV is already negligible and causes no degradation in the experiments. Therefore, V_D of 50 mV is more than safe to be utilized in the g_m measurements. In Fig. 6, each data point is calculated from at least five devices by dividing the average g_m with the certain chuck temperature by the g_m at that of 20 °C, and a minimum of 5 min is allowed after the environmental temperature becomes stable to ensure the preciseness. The error bars indicate 95% confidence intervals. Noticeably, the g_m of the TG In_2O_3 transistors degrades relatively slowly before 80 °C, and 90% or more of the g_m is preserved within this range. On the other hand, it decreases substantially after 100 °C, and only 35% is left at 160 °C. Applying this effect as a rough channel thermometer, the local temperature at the channel is less than 40 °C after the 1.8-V measurements at V_G of 4 V on a silicon substrate as exhibited in Fig. 5(e) and based on the estimation of Fig. 6; while it reduces to roughly 1 A/mm [I_D at $V_D = 1.8$ V of the first measurement

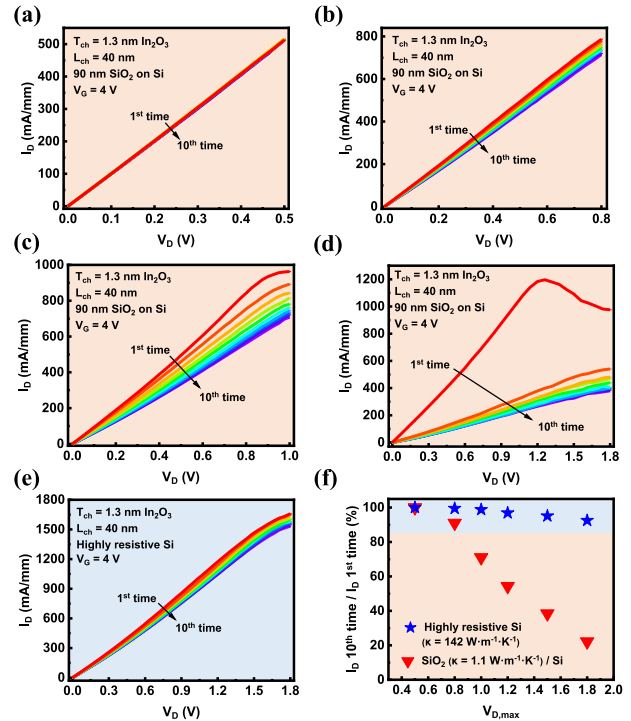


Fig. 5. I_D – V_D measurement of TG In_2O_3 transistors with (a) V_D up to 0.5 V and SiO_2/Si substrate, (b) V_D up to 0.8 V and SiO_2/Si substrate, (c) V_D up to 1 V and SiO_2/Si substrate, (d) V_D up to 1.8 V and SiO_2/Si substrate, and (e) V_D up to 1.8 V and highly resistive silicon substrate ten times in a row. (f) I_D preservation percentage between the first and tenth measurement with different V_D and substrates.

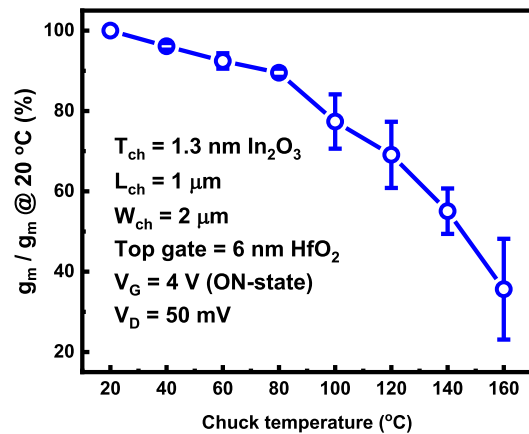


Fig. 6. g_m regression of TG In_2O_3 devices with long channels of 1 μm , low V_D of 50 mV, and ascending temperature up to 160 °C as an approximate channel thermometer.

in Fig. 5(d)] from 1.8 A/mm [I_D at $V_D = 1.8$ V on silicon in Fig. 4(d)]. 45% reduction in g_m and I_D refers to 140 °C device temperature from Fig. 6, which is significant. The evidential contrast specifies that the thermal engineering methodology does benefit the improved performance of the In_2O_3 TG transistors.

For high power density devices in general, substrates with even higher thermal conductivity might be desired. For instance, it is revealed that diamond ($\kappa = 1000$ – 2200 W·m⁻¹·K⁻¹ [22], [28]) as a substrate is capable of further profiting the performance of β - Ga_2O_3 -based power devices [22]. Nevertheless, the transparent body of diamond upraises the fabrication difficulties to a great extent, and its narrower commercial availability and much poorer affordability compared with a

wide variety of silicon restrict it from mass production. With moderate power density, TG In_2O_3 transistors with highly resistive silicon substrate are sufficient enough for dissipating the produced heat efficiently to avoid self-heating as previously presented and discussed, which makes it much more competitive in the realistic implementation and qualifies it in practical applications. For BEOL-compatible monolithic 3-D integration, high thermal conductive interlayer material is obviously desired for addressing thermal management issues.

IV. CONCLUSION

In summary, TG atomic-layer-thin In_2O_3 transistors on SiO_2/Si substrate or highly resistive silicon substrate are investigated. In the former case, a maximum I_D of 1 A/mm is achieved by scaling the L_{ch} down to 40 nm, and a low R_C of 0.24 $\Omega\cdot\text{mm}$ is obtained. By replacing the substrate with highly resistive silicon, the maximum I_D is elevated by approximately 100% to 2 A/mm. The significant improvement is due to the much higher thermal conductivity of silicon to dissipate the generated heat through the bottom substrate efficiently and mitigate the SHE. A quantitative study of the SHE on TG In_2O_3 devices is performed, and a rough thermometer based on the changes of the g_m under variant temperature is utilized to estimate the local temperature of In_2O_3 channels at ON-state. The current degradation rate with ascending temperature of silicon is less than 10% of SiO_2 , and the channel temperature is safely under 40 °C as highly resistive silicon serves as the substrate while up to 140 °C with SiO_2/Si substrate. Thermal engineering using high thermal conducting substrate or interlayer becomes critical for further exploration of In_2O_3 transistors with high current carrying capacity in practical monolithic 3-D integration applications.

REFERENCES

- [1] M. Si *et al.*, "Why In_2O_3 can make 0.7 nm atomic layer thin transistors," *Nano Lett.*, vol. 21, no. 1, pp. 500–506, Jan. 2021, doi: [10.1021/acs.nanolett.0c03967](https://doi.org/10.1021/acs.nanolett.0c03967).
- [2] M. Si, Z. Lin, A. Charnas, and P. D. Ye, "Scaled atomic-layer-deposited indium oxide nanometer transistors with maximum drain current exceeding 2 A/mm at drain voltage of 0.7 V," *IEEE Electron Device Lett.*, vol. 42, no. 2, pp. 184–187, Feb. 2021, doi: [10.1109/LED.2020.3043430](https://doi.org/10.1109/LED.2020.3043430).
- [3] M. Si, A. Charnas, Z. Lin, and P. D. Ye, "Enhancement-mode atomic-layer-deposited In_2O_3 transistors with maximum drain current of 2.2 A/mm at drain voltage of 0.7 V by low-temperature annealing and stability in hydrogen environment," *IEEE Trans. Electron Devices*, vol. 68, no. 3, pp. 1075–1080, Mar. 2021, doi: [10.1109/TED.2021.3053229](https://doi.org/10.1109/TED.2021.3053229).
- [4] S. Li *et al.*, "Nanometre-thin indium tin oxide for advanced high-performance electronics," *Nature Mater.*, vol. 18, no. 10, pp. 1091–1097, Oct. 2019, doi: [10.1038/s41563-019-0455-8](https://doi.org/10.1038/s41563-019-0455-8).
- [5] M. Si *et al.*, "Indium-tin-oxide transistors with one nanometer thick channel and ferroelectric gating," *ACS Nano*, vol. 14, no. 9, pp. 11542–11547, Sep. 2020, doi: [10.1021/acs.nano.0c03978](https://doi.org/10.1021/acs.nano.0c03978).
- [6] J. Wu, F. Mo, T. Saraya, T. Hiramoto, and M. Kobayashi, "A monolithic 3D integration of RRAM array with oxide semiconductor FET for in-memory computing in quantized neural network AI applications," in *Proc. IEEE Symp. VLSI Technol.*, Jun. 2020, pp. 1–2.
- [7] W. Chakraborty, B. Grisafe, H. Ye, I. Lightcap, K. Ni, and S. Datta, "BEOL compatible dual-gate ultra thin-body W-doped indium-oxide transistor with $I_{on}=370 \mu\text{A}/\mu\text{m}$, $SS=73 \text{ mV}/\text{dec}$ and I_{on}/I_{off} ratio $>4\times 10^9$," in *Proc. IEEE Symp. VLSI Technol.*, Jun. 2020, pp. 1–2.
- [8] S. Samanta, K. Han, C. Sun, C. Wang, A. V. Thean, and X. Gong, "Amorphous IGZO TFTs featuring extremely-scaled channel thickness and 38 nm channel length: Achieving record high $G_{m,max}$ of 125 $\mu\text{S}/\mu\text{m}$ at V_{DS} of 1 V and I_{ON} of 350 $\mu\text{A}/\mu\text{m}$," in *Proc. IEEE Symp. VLSI Technol.*, Jun. 2020, pp. 1–2.
- [9] K. Nomura, A. Takagi, T. Kamiya, H. Ohta, M. Hirano, and H. Hosono, "Amorphous oxide semiconductors for high-performance flexible thin-film transistors," *Jpn. J. Appl. Phys.*, vol. 45, no. 5, pp. 4303–4308, Apr. 2006, doi: [10.1143/JJAP.45.4303](https://doi.org/10.1143/JJAP.45.4303).
- [10] S. Fujita and K. Kaneko, "Epitaxial growth of corundum-structured wide band gap III-oxide semiconductor thin films," *J. Cryst. Growth*, vol. 401, pp. 588–592, Sep. 2014, doi: [10.1016/j.jcrysgro.2014.02.032](https://doi.org/10.1016/j.jcrysgro.2014.02.032).
- [11] H. Y. Kim *et al.*, "Low-temperature growth of indium oxide thin film by plasma-enhanced atomic layer deposition using liquid dimethyl(*N*-ethoxy-2,2-dimethylpropanamido)indium for high-mobility thin film transistor application," *ACS Appl. Mater. Interface*, vol. 8, no. 40, pp. 26924–26931, Oct. 2016, doi: [10.1021/acsami.6b07332](https://doi.org/10.1021/acsami.6b07332).
- [12] J. Lee *et al.*, "High mobility ultra-thin crystalline indium oxide thin film transistor using atomic layer deposition," *Appl. Phys. Lett.*, vol. 113, no. 11, Sep. 2018, Art. no. 112102, doi: [10.1063/1.5014029](https://doi.org/10.1063/1.5014029).
- [13] M. Si, Z. Lin, Z. Chen, and P. D. Ye, "First demonstration of atomic-layer-deposited BEOL-compatible In_2O_3 3D Fin transistors and integrated circuits: high mobility of 113 $\text{cm}^2/\text{V}\cdot\text{s}$, maximum drain current of 2.5 $\text{mA}/\mu\text{m}$ and maximum voltage gain of 38 V/V in In_2O_3 inverter," in *Proc. IEEE Symp. VLSI Technol.*, Jun. 2021, pp. 1–2.
- [14] R.-H. Yan, A. Ourmazd, and K. F. Lee, "Scaling the Si MOSFET: From bulk to SOI to bulk," *IEEE Trans. Electron Devices*, vol. 39, no. 7, pp. 1704–1710, Jul. 1992, doi: [10.1109/16.141237](https://doi.org/10.1109/16.141237).
- [15] H. Sakaki, T. Noda, K. Hirakawa, M. Tanaka, and T. Matsusue, "Interface roughness scattering in GaAs/AlAs quantum wells," *Appl. Phys. Lett.*, vol. 51, no. 23, pp. 1934–1936, Oct. 1987, doi: [10.1063/1.98305](https://doi.org/10.1063/1.98305).
- [16] A. Charnas, M. Si, Z. Lin, and P. D. Ye, "Realization of enhancement-mode atomic-layer thin In_2O_3 transistors with maximum current exceeding 2 A/mm at drain voltage of 0.7 V enabled by room temperature oxygen plasma treatment," *Appl. Phys. Lett.*, vol. 118, no. 5, Feb. 2021, Art. no. 052107, doi: [10.1063/5.0039783](https://doi.org/10.1063/5.0039783).
- [17] M. Si, Z. Lin, Z. Chen, and P. D. Ye, "High-performance atomic-layer-deposited indium oxide 3-D transistors and integrated circuits for monolithic 3-D integration," *IEEE Trans. Electron Devices*, early access, Aug. 25, 2021, doi: [10.1109/TED.2021.3106282](https://doi.org/10.1109/TED.2021.3106282).
- [18] M. H. Wong, Y. Morikawa, K. Sasaki, A. Kuramata, S. Yamakoshi, and M. Higashiwaki, "Characterization of channel temperature in Ga_2O_3 metal-oxide-semiconductor field-effect transistors by electrical measurements and thermal modeling," *Appl. Phys. Lett.*, vol. 109, no. 19, Nov. 2016, Art. no. 193503, doi: [10.1063/1.4966999](https://doi.org/10.1063/1.4966999).
- [19] R. J. Trew, D. S. Green, and J. B. Shealy, "AlGaIn/GaN HFET reliability," *IEEE Microw. Mag.*, vol. 10, no. 4, pp. 116–127, Jun. 2009, doi: [10.1109/MMM.2009.932286](https://doi.org/10.1109/MMM.2009.932286).
- [20] R. Gaska, A. Osinsky, J. W. Yang, and M. S. Shur, "Self-heating in high-power AlGaIn-GaN HFETs," *IEEE Electron Device Lett.*, vol. 19, no. 3, pp. 89–91, Mar. 1998, doi: [10.1109/55.66174](https://doi.org/10.1109/55.66174).
- [21] Y. Zhou *et al.*, "Thermal characterization of polycrystalline diamond thin film heat spreaders grown on GaN HEMTs," *Appl. Phys. Lett.*, vol. 111, no. 4, Jul. 2017, Art. no. 041901, doi: [10.1063/1.4995407](https://doi.org/10.1063/1.4995407).
- [22] J. Noh *et al.*, "High performance $\beta\text{-Ga}_2\text{O}_3$ Nano-membrane field effect transistors on a high thermal conductivity diamond substrate," *IEEE J. Electron Devices Soc.*, vol. 7, pp. 914–918, 2019, doi: [10.1109/JEDS.2019.2933369](https://doi.org/10.1109/JEDS.2019.2933369).
- [23] H. R. Shanks, P. D. Maycock, P. H. Sidles, and G. C. Danielson, "Thermal conductivity of silicon from 300 to 1400°K," *Phys. Rev.*, vol. 130, pp. 1743–1748, Jun. 1963, doi: [10.1103/PhysRev.130.1743](https://doi.org/10.1103/PhysRev.130.1743).
- [24] M. B. Kleiner, S. A. Kuhn, and W. Weber, "Thermal conductivity measurements of thin silicon dioxide films in integrated circuits," *IEEE Trans. Electron Devices*, vol. 43, no. 9, pp. 1602–1609, Sep. 1996, doi: [10.1109/16.535354](https://doi.org/10.1109/16.535354).
- [25] A. Pérez-Tomás *et al.*, "Temperature impact and analytical modeling of the AlGaIn/GaN-on-Si saturation drain current and transconductance," *Semicond. Sci. Technol.*, vol. 27, no. 12, Oct. 2012, Art. no. 125010, doi: [10.1088/0268-1242/27/12/125010](https://doi.org/10.1088/0268-1242/27/12/125010).
- [26] J. Kuzmík, P. Javorka, A. Alam, M. Marso, M. Heuken, and P. Kordoš, "Determination of channel temperature in AlGaIn/GaN HEMTs grown on sapphire and silicon substrates using DC characterization method," *IEEE Trans. Electron Devices*, vol. 49, no. 8, pp. 1496–1498, Aug. 2002, doi: [10.1109/TED.2002.801430](https://doi.org/10.1109/TED.2002.801430).
- [27] A. K. Goel and T. H. Tan, "High-temperature and self-heating effects in fully depleted SOI MOSFETs," *Microelectron. J.*, vol. 37, no. 9, pp. 963–975, Sep. 2006, doi: [10.1016/j.mejo.2006.01.006](https://doi.org/10.1016/j.mejo.2006.01.006).
- [28] J. R. Olson, R. O. Pohl, J. W. Vandersande, A. Zoltan, T. R. Anthony, and E. F. Banholzer, "Thermal conductivity of diamond between 170 and 1200 K and the isotope effect," *Phys. Rev. B, Condens. Matter*, vol. 47, no. 22, pp. 14850–14857, Jun. 1993, doi: [10.1103/PhysRevB.47.14850](https://doi.org/10.1103/PhysRevB.47.14850).
- [29] G. K. Reeves and H. B. Harrison, "Obtaining the specific contact resistance from transmission line model measurements," *IEEE Electron Device Lett.*, vol. EDL-3, no. 5, pp. 111–113, May 1982, doi: [10.1109/EDL.1982.25502](https://doi.org/10.1109/EDL.1982.25502).